Book Section:

Crowther, P.A., Lennon, D.J., Walborn, N.R. et al. (1 more author) (2008) Properties of Galactic B supergiants. In: Mass Loss from Stars and the Evolution of Stellar Clusters. Astronomical Society of the Pacific Conference Series (388). Astronomical Society of the Pacific , p. 109. ISBN 978-1-58381-644-8

eprints@whiterose.ac.uk
https://eprints.whiterose.ac.uk/

Properties of Galactic B supergiants

Paul A. Crowther

*Dept of Physics & Astronomy, University of Sheffield, Hounsfield Rd,
She ffield, S3 7RH, UK*

Daniel J. Lennon

*Isaac Newton Group, Apartado 321, 38700 Santa Cruz de La Palma,
Canary Islands, Spain*

Nolan R. Walborn

*Space Telescope Science Institute, 3700 San Martin Drive, Baltimore
MD 21218, USA*

Stephen J. Smartt

*Department of Physics and Astronomy, Queen's University Belfast,
Belfast BT7 1NN, UK*

Abstract. Physical and wind properties of Galactic B supergiants are presented based upon non-LTE line blanketed model atmospheres, including Sher 25 toward the NGC 3603 cluster. We compare Hα derived wind densities with recent results for SMC B supergiants and generally confirm theoretical expectations for stronger winds amongst Galactic supergiants. Mid B supergiant winds are substantially weaker than predictions from current radiatively driven wind theory, a problem which is exacerbated if winds are already clumped in the Hα line forming region. We find that the so-called 'bistability jump' at B1 ($T_{\rm eff}$ $\sim$ 21kK) from Lamers et al. is rather a more gradual downward trend. CNO elemental abundances, including Sher 25, reveal partially processed material at their surfaces. In general, these are in good agreement with evolutionary predictions for blue supergiants evolving redward accounting for rotational mixing. A few cases, including HD 152236 (ζ^1 Sco), exhibit strongly processed material which is more typical of Luminous Blue Variables. Our derived photospheric [N/O] ratio for Sher 25 agrees with that for its ring nebula, although a higher degree of CNO processing would be expected if the nebula originated during a red supergiant phase, as is suspected for the ring nebula ejected by the B supergiant progenitor of SN 1987A, Sk–69° 202. Sher 25 has an inferred age of $\sim$5Myr in contrast with $\sim$2Myr for HD 97950, the ionizing cluster of NGC 3603, so it may be a foreground object or close binary evolution may be responsible for its unusual location in the H-R diagram.

1. Introduction

O stars dominate the energetics of young starbursts since their ionizing output is a very steep function of effective temperature (Leitherer et al. 1992). As such, numerous intensive studies of O stars in the Milky Way and Magellanic

Clouds have been undertaken, with regard to determining their fundamental parameters and the empirical dependence of their wind strengths on metallicity (e.g. Mokiem et al. 2006ab). Unfortunately, O dwarfs are visually faint in external galaxies due to their large bolometric corrections and small radii, with typically M_V = -5.0 mag. O star abundances of CNO elements are difficult to derive (Crowther et al. 2002), yet these are sensitive to early rotational mixing (e.g. Meynet & Maeder 2000).

In contrast, B supergiants have received rather less attention since they are less relevant for energetics of young starbursts. Nevertheless, they are visually bright, typically $M_V = -7.0$ mag, possess larger radii and so are easy to observe individually in nearby galaxies, permitting robust tests of the metallicity dependence of radiatively driven wind theory, which is predicted to increase from early to mid B supergiants (Vink et al. 2000). In addition, CNO abundances are readily obtained from optical spectroscopy, for comparison to evolutionary model predictions. Notably, Trundle et al. (2004) and Trundle & Lennon (2005) have studied a large sample of SMC B supergiants using the line blanketed version of FASTWIND (Puls et al. 2005). To date, the most extensive study of Galactic B supergiants is by Kudritzki et al. (1999), who adopted the T_{eff} scale from the plane-parallel unblanketed study of McErlean et al. (1999), plus mass-loss rates from the unblanketed version of FASTWIND.

Our present study of Galactic B supergiants employs CMFGEN (e.g. Hillier et al. 2003) which also incorporates line blanketing and spherical geometry, and so permits a direct comparison with recent SMC results, plus CNO abundance determinations. Do the abundances of normal B supergiants match those of stars evolving towards red supergiants (RSG) or returning from RSG following convective dredge-up? Comparisons with Luminous Blue Variables (LBVs) are also made, since they exhibit spectral characteristics of early B supergiants at visual minimum and A supergiants at visual maximum (Crowther 1997). Notably, ζ^1 Sco (HD 152236) is an early B hypergiant and lies above the empirical Humphreys-Davidson limit (Humphreys & Davidson 1979). We also include new stellar and nebular studies of Sher 25 (Hendry et al. 2006), an apparently normal B supergiant in the giant HII region NGC 3603 yet possessing an ejecta nebula reminiscent of that associated with SN 1987A (Brandner et al. 1997b).

Finally, we consider the empirical bistability jump amongst early B supergiants, which was originally developed for the LBV P Cygni by Pauldrach & Puls (1990), in the sense that slight variations in its effective temperature resulted in hydrogen being ionized or neutral in its outer stellar wind (Najarro et al. 1997). Lamers et al. (1995) studied wind velocities of OB stars, and established a discontinuity in the ratio of v_∞ to v_{esc} for B0.5 and B1 supergiants, which is assumed in current stellar wind models of Vink et al. (2000).

2.   Observations and analysis

Full details of observations and method of analysis are presented by Crowther et al. (2006). In summary we have observed 26 Galactic early-type Ia supergiants – spanning the spectral range O9.5 to B3 – at intermediate dispersion in the blue and red using the 1.0m JHK, 2.5m INT or 4.2m WHT for the northern sample or at the 1.5m CTIO for the southern sample, with the exception of Sher 25
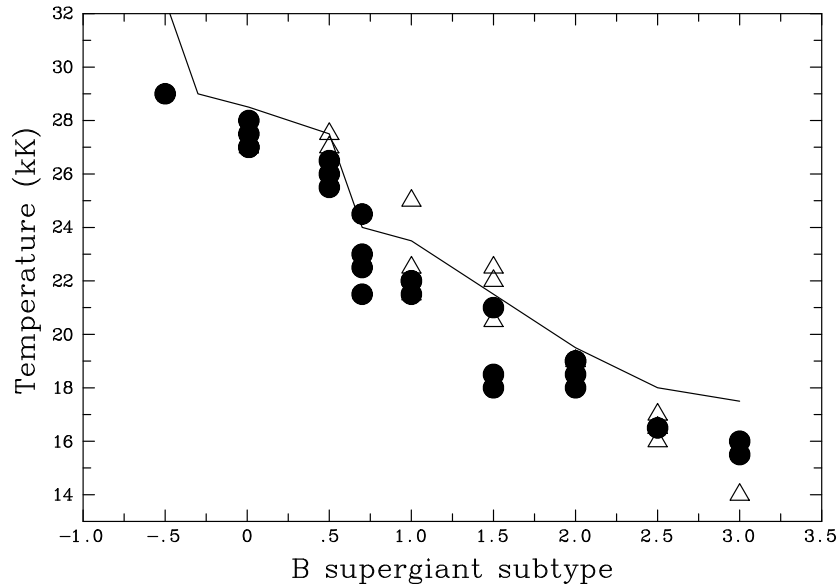
Figure 1. Temperature scale of B supergiants from this Milky Way study (CMFGEN, circles) plus Trundle et al. (2004) and Trundle & Lennon (2005) for the SMC (FASTWIND, triangles) versus the McErlean et al. (1998, solid line) calibration.

for which 3.9m AAT echelle spectroscopy was obtained. Cluster or association distance estimates are available for 75% of the sample, whilst average subtype absolute magnitudes are taken from Magellanic Cloud stars for the remainder. For the case of Sher 25, we adopt a distance of 7.9 kpc (Russeil 2003) towards NGC 3603 from which we obtain $M_V = -7.4$ mag.

For the present study we have used CMFGEN (see Hillier et al. 2003) which solves the radiative transfer equation in the co-moving frame, under the constraints of radiative and statistical equilibrium. For the supersonic part, the velocity is parameterized with a classical β law, which is connected to a hydrostatic density structure at depth using a H-He TLUSTY model. A depth independent Doppler profile was assumed for the atmospheric structure calculation in the co-moving frame, whilst a radially dependent turbulence was used to calculate the emergent spectrum in the observer's frame, in which incoherent electron scattering and Stark broadening for H, He were included.

Stellar temperatures were derived from suitable lines of HeI-II (O9.5-B0), SiIII–IV (B0.5–B2), SiII-III (B2.5-B3) such that radii and luminosities followed from absolute magnitudes, with Hα observations providing $\dot{M}$ and the velocity exponent β. Terminal velocities and rotational velocities were taken from Howarth et al. (1997). H/He abundances are difficult to accurately derive in B supergiants, such that He/H=0.2 by number is adopted throughout. CNO abundances were varied to reproduce the relevant optical absorption lines, and compared with Solar abundances (Asplund et al. 2004).
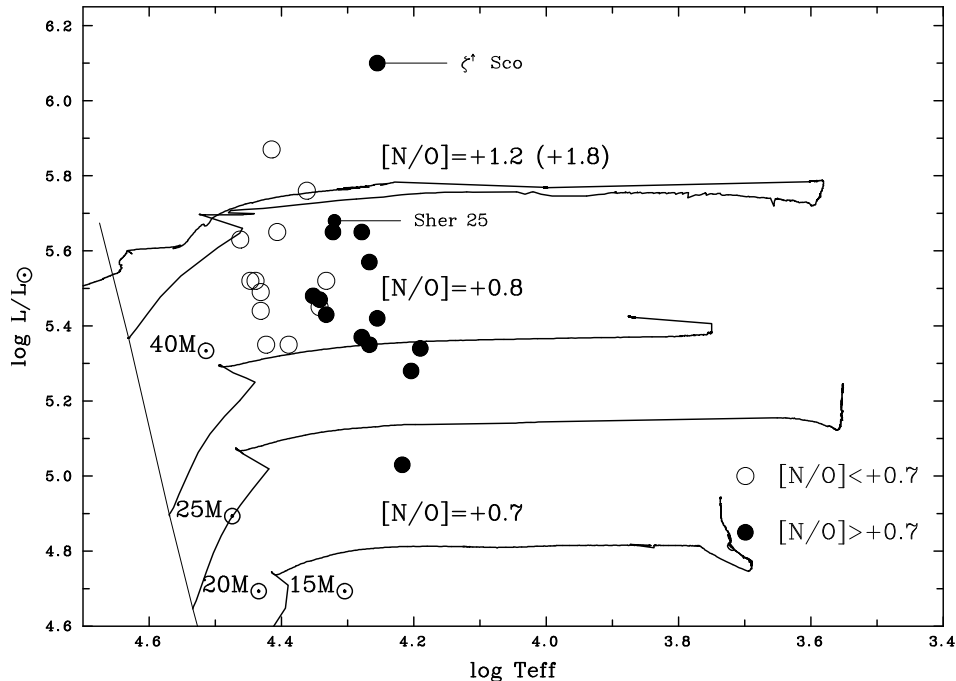
Figure 2.   Observed H-R diagram for our sample of B supergiants, coded by their degree of N/O enrichment, together with tracks from Solar metallicity, rotating (v_{init}=300 km sec^{-1}) evolutionary models (dotted lines) from Meynet & Maeder (2000) for which predicted N/O enrichments are indicated for redward (blueward) evolution at T_{eff} = 22kK. The location of Sher 25 and HD 152236 (ζ^1 Sco) are indicated.

3.   Physical and Wind Properties

3.1.   Temperature scale

The inclusion of line blanketing and spherical geometry into O star models has resulted in a major 15±5% downward revision in their T_{eff} spectral type calibration (Crowther et al. 2002; Martins et al. 2005). For B supergiants, we present our results together with those of Trundle et al. (2004) and Trundle & Lennon (2005) for SMC stars studied with FASTWIND (Puls et al. 2005) in Fig. 1, together with the results from unblanketed plane parallel models of McErlean et al. (1999). As is apparent, the revision in B supergiant temperature scale is modest, with typical revisions of -1 to -2kK. Note that results for line blanketed versions of CMFGEN and TLUSTY are consistent to within ±0.5kK for several stars in common between the present study and Urbaneja (2004).

The location of our stars in the H-R diagram is presented in Fig. 2, such that the majority are consistent with initial masses in the range 20–40 $M_{\odot}$, whilst ζ^1 Sco is rather more massive. Spectroscopically derived masses span a wide range, from 8 up to 76 $M_{\odot}$, based upon surface gravities reliable to log g $\pm$ 0.15 dex. In most cases spectroscopic masses are lower than those estimated

from evolutionary models, indicating another example of a 'mass discrepancy', in common with Trundle & Lennon (2005).
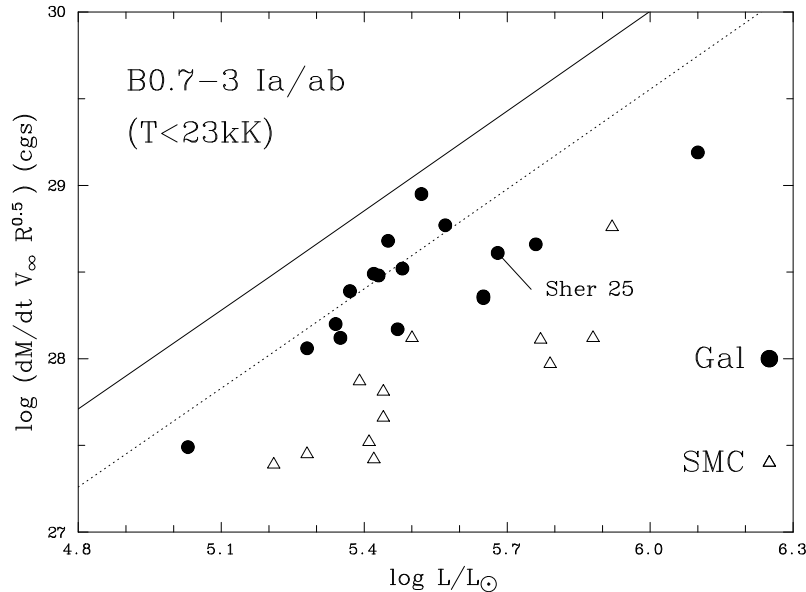

Figure 3.   Comparison between the wind momenta of Galactic B0.7–3 supergiants ($T_{\rm eff}$ ≤23kK) and studies of SMC counterparts Trundle et al. 2004; Trundle & Lennon 2005), assuming homogeneous Hα mass-loss rates, plus radiatively driven wind theory predictions by Vink et al. (2000, 2001) for the Milky Way (solid) and SMC (dotted). Sher 25 is indicated, revealing wind properties typical of Galactic B supergiants.

3.2.   Mass-loss rates

Hα mass-loss rates compare well with mid-IR excess methods (e.g. Barlow & Cohen 1977) and line blanketed FASTWIND models (Urbaneja 2004), but exceed those derived by Kudritzki et al. (1999) by a factor of three, who used an unblanketed version of FASTWIND for B2–3 supergiants. Spectroscopic studies in which clumped winds are included tend to produce superior spectral fits to far-UV lines (Evans et al. 2004b), suggesting comparable clumping factors for the inner (Hα line) and outer (mid-IR continuum) forming regions.

   In general, wind momenta of Galactic B0–0.5 subtypes lie close to the Vink et al. (2000) prediction. If winds of early B supergiants are clumped in the Hα line forming region, we would need to shift the observed wind momenta to lower values. Fig. 3 presents wind momenta for Galactic B0.7–3 supergiants ($T_{\rm eff}$ (≤ 23kK) together with corresponding SMC results from Trundle et al. (2004) and Trundle & Lennon (2005), plus theoretical predictions from Vink et al. (2000, 2001). A clear separation between Galactic and SMC supergiants is apparent, with approximately the offset predicted by Vink et al. (2001). However, measured values lie typically ∼0.5 dex below the Vink et al. calibration. As discussed above, if Hα derived mass-loss rates of OB stars need to be corrected for

clumped winds, as suggested by recent observational evidence, including Evans
et al. (2004b) for B supergiants, the difference between theory and observation
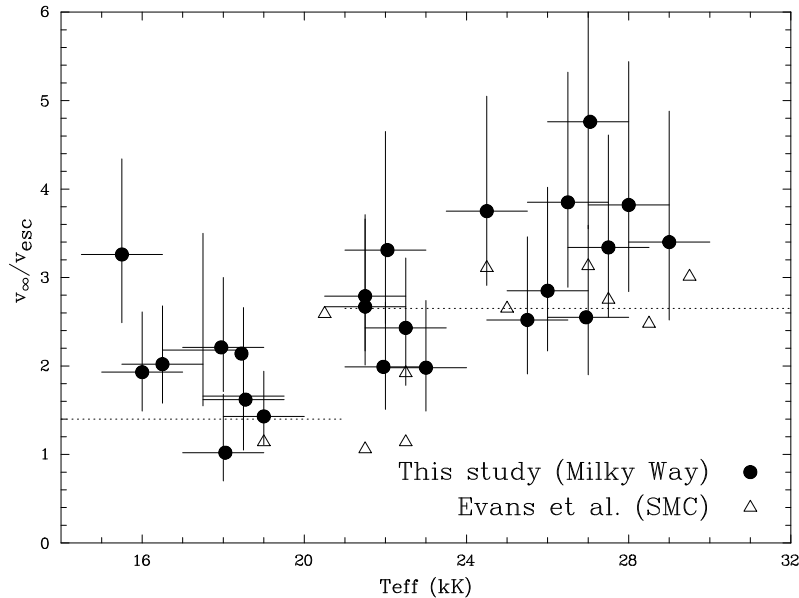would be further exacerbated.

Figure 4.   The ratio $v_\infty/v_{\rm esc}$ as a function of effective temperature for Galac-
tic B supergiants from the present study (filled circles), together with results
from Evans et al. (2004a, open triangles) for SMC B supergiants. Error bars
relate to uncertainties in temperature (± 1 kK), gravity (± 0.15 to 0.2 dex)
and absolute magnitude (± 0.3 to 1 mag).

3.3.   Bistability jump

In Fig. 4 we present our current results, together with values from Evans et al.
(2004a), based on measured HST/STIS wind velocities, plus model atmosphere
results from Evans et al. (2004b), Trundle et al. (2004), Trundle & Lennon
(2005). In contrast with the discontinuity identified by Lamers et al. (1995), we
identify a gradual downward trend of v_∞ / $v_{\rm esc}$ with temperature, albeit with
a large scatter. For $T_{\rm eff} > 24$kK (approximately B0.5 Ia and earlier), v_∞ / $v_{\rm esc}$
~ 3.4, for 20kK$\leq T_{\rm eff} \leq$24kK (approximately B0.7–1 Ia) v_∞ / $v_{\rm esc} \sim 2.5$, and for
$T_{\rm eff} < 20$kK (approximately B1.5 Ia and later) v_∞ / $v_{\rm esc} \sim 1.9$. This reveals that
the B1 'jump' is misleading in the context of normal B supergiants. Prinja &
Massa (1998) came to similar conclusions based on a larger B supergiant sample,
albeit with an adopted subtype-temperature calibration.

      Empirical values of the Lamers et al. (1995) 'bistability jump' were adopted
by Vink et al. (2000) in their radiatively driven wind calculations. These pre-
dictions have subsequently been used in evolutionary models (e.g. Meynet &
Maeder 2000). Consequently, our re-determination of physical parameters and
wind properties of early B supergiants has potential consequences for evolution-
ary and spectral synthesis calculations.

3.4. Photospheric CNO abundances

Fig. 5 provides a summary of our derived CNO abundances. With respect to the current Solar values (Asplund et al. 2004), carbon is depleted by 0.4±0.4 dex, oxygen is mildly depleted by up to 0.5 dex, whilst nitrogen is enriched by 0.6±0.4 dex. Mean [N/C] and [N/O] ratios indicate evidence for partial CNO processing within the photospheres of B supergiants. Our results support previous abundance estimates from the literature, which were typically based upon differential abundance analyses from plane-parallel LTE or non-LTE model atmospheres.

On average, the observed degree of CNO processing agrees well with recent evolutionary models for 20–$40 M_\odot$, for which [N/C] = +0.8 to +1.3 and [N/O] = +0.7 to +1.2 were predicted via rotational mixing ($v_{\rm init}$ = 300 km sec^{-1}) at $\sim$22kK on the redward evolutionary track (Meynet & Maeder 2001). Spectroscopically, all our sample of supergiants are morphologically normal, except for κ Cas (HD 2905, BC 0.7Ia) which indeed possesses the lowest N enrichment in our sample with [N/O] = +0.1 dex. Conversely, ζ^1 Sco (HD 152236, B1.5 Ia$^+$), one of two hypergiants in our sample, possesses the highest N enrichment of [N/O] = +1.3, that is more typical of nebulae associated with Luminous Blue Variables, e.g. [N/O] = +1.3 to +1.9 dex for AG Car and R127 (Lamers et al. 2001).

4. Sher 25 in NGC 3603

Sher 25 (B1.5 Iab, Moffat 1983) is associated with a ring nebula and apparent bipolar outflows (Brandner et al. 1987a). The ring nebula is reminiscent of the inner nebula associated with SN 1987A, which is presumed to have been ejected from the Sk–69° 202 (B3 I, Walborn et al. 1989) progenitor. Both nebulae share physical sizes of $\sim$0.5 pc, with dynamical ages of several thousand years and apparent nitrogen enrichment (Panagia et al. 1996; Brandner et al. 1997b). Hendry et al. (2006) present studies of the ring nebula and bipolar lobes from Sher 25, plus that of the giant HII region NGC 3603 toward which Sher 25 is located.

The stellar and wind properties of Sher 25 are typical of other Galactic early B supergiants in our sample (recall Figs. 2–3), as derived from optical AAT/UCLES spectroscopy, i.e. $T_{\rm eff}$ = 21kK, log $L_\star$ / $L_\odot$ = 5.68, $\dot{M}$ = 1.2×10^{-6} $M_\odot$yr^{-1} $v_\infty \approx$ 750 km sec^{-1} using a distance of 7.9 kpc (Russeil 2003). The surface elemental abundances of Sher 25 derived here, [N/C]=+1.3 and [N/O]=+1.2, are compared with other B supergiants in Fig. 5. Table 1 provides a comparison with previous photospheric derivations (Smartt et al. 2002) plus ring nebula and bipolar lobe abundances in Table 1. Note that our derived [N/O] ratio agrees perfectly with the mean nebular ratio from Hendry et al. (2006), whilst the giant HII region is close to Solar composition (see also Esteban et al. 2005).

If we compare the location of Sher 25 in the H-R diagram with evolutionary models of Meynet & Maeder (2000) it lies close to an initial $40 M_\odot$ rotating with $v_{\rm init}$ = 300 km sec^{-1} (recall Fig. 2). If we adjust the predictions from Meynet & Maeder to the Solar abundances from Asplund et al. (2004) one expects
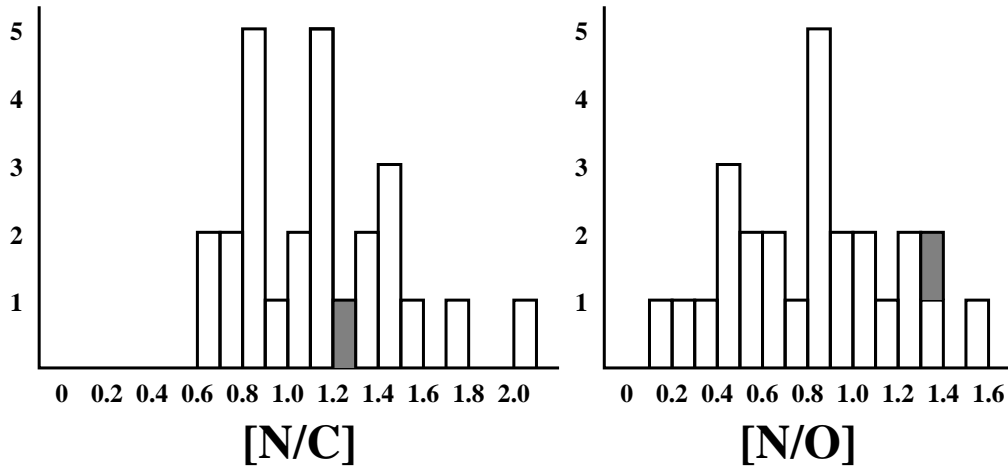
Figure 5.   [N/C] (left) and [N/O] (right) abundances for Milky Way B supergiants from the present CMFGEN study (relative to Asplund et al. 2004), typically revealing partially CNO processed material, in which Sher 25 is indicated in grey. Although the relative abundances presented here are anticipated to be robust, there remains considerable absolute uncertainty, since results for a subset of the present sample using FASTWIND differ by up to 0.5 dex (Urbaneja 2004).

a nitrogen enhancement of +1.0 dex and oxygen depletion of –0.2 dex on the redward track after 5.1 Myr, i.e. [N/O] = +1.2 dex, in perfect agreement with the mean nebular and stellar CMFGEN results. For the post-RSG stage after 5.2 Myr, [N/O] = +1.8 dex is predicted. Consequently, Sher 25 is consistent with a single star evolving towards the RSG phase.

However, amongst the most successful models to explain SN 1987A during its B supergiant phase are those of Podsiadlowski (1992), involving either accretion from, or merger with, a binary companion during the common envelope evolution in the RSG stage of Sk–69° 202. Assuming membership of NGC 3603, Sher 25 is more luminous than Sk–69° 202 – for which $\log L_\star / L_\odot \sim 5.1$. If Sher 25 has undergone a similar evolution, which may be suggested from its recent nebular ejection, this star would not be expected to possess CNO abundances typical of normal B supergiants evolving towards the RSG phase. The dynamical age of the ring nebula and bipolar lobes is ∼8700 yr (Brandner et al. 1997b, adjusted for a distance of 7.9 kpc).

One final puzzle regarding Sher 25 is that it lies only 20 arcsec (1 pc) in projection from the central ionizing cluster, HD 97950, in NGC 3603, yet its inferred age of ∼5Myr greatly exceeds that of HD 97950 which is ∼2Myr (Crowther & Dessart 1998). HD 97950 closely resembles R136 in the LMC (Walborn 1973; Moffat 1983), yet unlike R136, it does not possess an extensive halo of earlier phases of massive star formation. Perhaps Sher 25 is a foreground object, which may plausibly be inferred from the presence of other stars which are older than the HD 97950 cluster to one side (Brandner et al. 1997a). In this case the stellar luminosity and the size of the ring nebula are smaller than

adopted here, although we note its physical and wind properties are typical of other Galactic early B supergiants. Alternatively, close binary evolution may be responsible for its unusual position in the H-R diagram.

Table 1.   Photosphere abundances of Sher 25, together with nebular abundances for the ejecta nebula and NGC 3603 HII region, with reference to Solar abundances of log(O/H)+12=8.66 and log(N/H)+12=7.78 from Asplund et al. (2004).

	log O/H +12	log N/H +12	[N/O]	Reference
Star (CMFGEN)	8.14	8.48	1.2	This study
Star (TLUSTY)	8.87	8.42	0.4	Smartt et al. 2002
Ring nebula	8.55	8.97	1.3	Hendry et al. 2006
Bipolar lobes	8.64	8.88	1.1	Hendry et al. 2006
HII region	8.56	7.47	−0.1	Hendry et al 2006

References

Asplund M. Grevesse N. Sauval A.J. et al. 2004, A&A 417, 751
Barlow M.J., Cohen M., 1977, ApJ 213, 737
Brandner W., Grebel E.K., Chu Y.-H., Weis K., 1997a ApJ 475, L45
Brandner W., Chu Y.-H., Eissenhauer F., Grebel E.K., Points S.D., 1997b ApJ 489, L153
Crowther P.A. 1997, in: Luminous Blue Variables: Massive Stars in Transition, A Nota & H.J.G.L.M. Lamers (eds)., ASP Conf Ser 120, p.51
Crowther P.A., Dessart L., 1998, MNRAS 296, 622
Crowther P.A., Hillier D. J., Evans C. J. et al., 2002, ApJ, 579, 774
Crowther P.A., Lennon D.J., Walborn N.R., 2006, A&A 446, 279
Esteban C., Garcia-Rojas J., Peimbert M. et al. 2005, ApJ 618, L95
Evans C.J. Lennon D.J., Trundle C., Heaps S.R., Lindler D.J., 2004a, ApJ 607, 451
Evans C.J., Crowther P.A., Fullerton A.W., Hillier D.J., 2004b, ApJ 610, 1021
Hendry M.A., Smartt S.J., Skillman E.D., Evans C.J., 2006, MNRAS in preparation
Hillier D. J., Lanz T., Heap S. R. et al., 2003, ApJ 588, 1039
Howarth I.D., Siebert K.W., Hussain G.A.J., Prinja R.K., 1997, MNRAS 284, 265
Humphreys R.M., Davidson K., 1979, ApJ 232, 409
Kudritzki R-P., Puls J., Lennon D. J. et al., 1999, A&A, 350, 970
Lamers H.J.G.L.M., Snow T.P., Lindholm D.M. 1995, ApJ 455, 269
Lamers H.J.G.L.M., Nota A., Panagia N., Smith L.J., Langer N., 2001, ApJ 551, 764
Leitherer C., Robert C., Drissen L., 1992 ApJ 401, 596
Lanz T., Hubeny I., 2003, ApJS 146, 417
Martins F., Schaerer D., Hillier D.J., 2005, A&A 436, 1049
McErlean N.D., Lennon D.J., Dufton P. L., 1999, A&A 349, 553
Meynet G., Maeder A., 2000, A&A 361, 159
Moffat A.F.J., 1983, A&A 123, 273
Mokiem R., de Koter A., Evans C.J. et al. 2006a, A&A in press (astro-ph/0606403)

Mokiem R., de Koter A., Evans C.J. et al. 2006b, A&A to be submitted

Najarro F., Hillier D.J., Stahl O., 1997, A&A 326, 1117

Panagia N., Scuderi S., Gilmozzi R., Challis P.M., Garnavich P.M., Kirshner R.P., 1996, ApJ 459, L17

Pauldrach A.W., Puls J. 1990, A&A 237, 409

Podsiadlowski P., 1992, PASP 104, 717

Prinja R.K., Massa D., 1998, in Boulder-Munich II: Properties of Hot Luminous Stars (ed. Howarth I.D.), ASP Conf Ser 131, p.218

Puls J., Urbaneja M.A., Venero R., Repolust T., Springmann U., Jokuthy A., Mokiem M.R. 2005, A&A 435, 669

Russeil D., 2003, A&A 397, 133

Smartt S.J., Lennon D.J., Kudritzki R.P., Rosales F., Ryans R.S.I., Wright N., 2002, A&A 391, 979

Trundle C., Lennon D.J. 2005, A&A 434, 677

Trundle C., Lennon D.J., Puls J., Dufton P.L., 2004, A&A 417, 217

Urbaneja M., 2004, PhD thesis, University of La Laguna (IAC), Spain

Vink J.S., de Koter A., Lamers H.J.G.L.M., 2000, A&A 362, 295

Vink J.S., de Koter A., Lamers H.J.G.L.M., 2001, A&A 369, 574

Walborn N.R., 1973, ApJ 182, L21

Walborn N.R., Prevot M.L., Prevot L., Wamsteker W., Gonzalez R. Gilmozzi R., Fitzpatrick E.L. 1989, A&A 219, 229